

RESEARCH ARTICLE

Fog trends in India: Relationships to fog type and western disturbances

Daniel K. E. Smith¹  | Stephen R. Dorling¹ | Ian A. Renfrew¹  |
Andrew N. Ross² | Craig Poku²

¹School of Environmental Sciences,
University of East Anglia, Norwich, UK

²School of Earth and Environment,
University of Leeds, Leeds, UK

Correspondence

Daniel K. E. Smith, School of
Environmental Sciences, University of
East Anglia, Norwich Research Park,
Norwich NR4 7TJ, UK.
Email: d.smith5@uea.ac.uk

Funding information

Newton Fund, Grant/Award Number:
WCSSP India WP2 Lot 2

Abstract

Fog is a major hazard in wintertime over India, particularly in the Indo-Gangetic Plains, leading to significant impacts for transport and human health. Using 3-hourly surface observations, from 69 sites across India, all fog and dense fog events between 2000 and 2020 are identified. For each event, the main fog formation mechanism is objectively categorized using a classification algorithm, distinguishing between radiation, advection, evaporation, precipitation or cloud-base lowering fog types. In contrast to the findings of other international studies, radiation fog dominates as the most common fog type at the vast majority of locations in India, accounting for 68.1% of all fog events and 70.0% of dense fog events. Statistically significant positive trends are seen in the frequency of all fog events at Delhi, Lucknow and Patna, in the Indo-Gangetic plains, between 1997/1998 and 2018/2019, dominated by comparable statistically significant positive trends in radiation fogs. Western disturbances (WD) are often linked to the formation of fog in India. Using a climatology of WDs, we show that 46.9% of radiation fog onsets in Delhi in December and January, the primary fog months, happened in conjunction with an active WD event. Conversely, only 32.3% of WDs during these same months coincided with the onset of a radiation fog event. WD-related radiation fog events are shown to cluster into three distinct groups, with WD centres located to the northwest (51.4% of cases), southwest (13.3%) and east (35.2%) of Delhi. Each cluster is shown to have coherent and distinct near-surface characteristics which are conducive to fog formation. Trends in WD frequency cannot fully account for the observed trends in fog events. We argue that the fog trends are more likely the result of a complex interaction between urban expansion and the associated rapid change in aerosol loading, resulting in impacts on radiation balance, microphysics and heat-island processes.

KEYWORDS

fog, fog trends, fog type, India, visibility, western disturbance

This is an open access article under the terms of the [Creative Commons Attribution](https://creativecommons.org/licenses/by/4.0/) License, which permits use, distribution and reproduction in any medium, provided the original work is properly cited.

© 2022 The Authors. *International Journal of Climatology* published by John Wiley & Sons Ltd on behalf of Royal Meteorological Society.

1 | INTRODUCTION

Over 11,000 people died in India in 2017 as a result of fog-related road traffic accidents (Kapoor, 2019). Indeed, on a global basis, fog poses a significant hazard for both road transport (Ashley *et al.*, 2015) and aviation, representing the second most likely cause of weather-related aviation accidents behind strong winds (Gultepe *et al.*, 2019). Fog is particularly frequent over northern India, where 48 fog days a year are observed on average (Ghude *et al.*, 2017). These fog events mainly occur in winter (Srivastava *et al.*, 2017; Shrestha *et al.*, 2018), in particular December and January when 66% of fog days occur (Srivastava *et al.*, 2016). Economically, fog impacts were especially severe during the winter of 2013–2014 in northern India, when the aviation sector recorded losses of \$1.78 million at the IGI airport in Delhi alone (Kulkarni *et al.*, 2019). Fog is a reduction in visibility to below 1 km due to cloud droplets near the Earth's surface, with this reduction in visibility considered its greatest hazard. However, prolonged fog events are also associated with poor air quality episodes, specifically high sulphate aerosol concentrations, impacting human health (Hameed *et al.*, 2000), and with declines in wheat productivity in the northern plains of India (Singh and Singh, 2010).

It is particularly concerning then that northern India and surrounding regions have experienced a recent (1980–2016) increase in fog frequency, persistence and intensity (Jenamani, 2007; 2012; Syed *et al.*, 2012; Srivastava *et al.*, 2016; Ghude *et al.*, 2017; Shrestha *et al.*, 2018; Hingmire *et al.*, 2019). The increasing trend in fog frequency in the recent era is almost unique to the region, inland eastern-central China being one of the only other areas to have experienced an increase over a similar period (Niu *et al.*, 2010). Decreasing trends in fog frequency have been widely observed; for example, in Los Angeles, CA (Witiw and LaDochy, 2008), Brazil (Gonçalves *et al.*, 2008), Europe (Vautard *et al.*, 2009), South Korea (Belorid *et al.*, 2015), Japan (Sugimoto *et al.*, 2013; Akimoto and Kusaka, 2015) and Shanghai, China (Gu *et al.*, 2019). The drivers of fog trends involve complex interactions and feedbacks between many processes at different scales. Important drivers of fog frequency trends include changes to the synoptic-scale circulation (Witiw and LaDochy, 2008; Sugimoto *et al.*, 2013), local land use changes such as urban expansion (Belorid *et al.*, 2015; Gu *et al.*, 2019) and changes in atmospheric composition through patterns of air pollution (Vautard *et al.*, 2009; Niu *et al.*, 2010). Urban expansion has two counter-acting impacts on fog frequency: the larger urban heat island effect increases temperature which decreases fog frequency, whereas an increase in

air pollution may increase fog frequency. Urban expansion results in land use change and an increase in surface roughness, reducing average wind speeds, which could by themselves, ignoring any potential accompanying changes in temperature and humidity, increase fog frequency. Klemm and Lin (2016) postulated that NO_x and SO₂ emissions and concentrations were correlated with fog intensity as these are precursors for small, hygroscopic particles that can form fog droplets. Indeed, other studies such as Vautard *et al.* (2009) and Jenamani (2007) find SO₂ emissions and NO_x concentration trends, respectively, correlate with fog frequency.

In northern India, many urban areas have undergone rapid expansion. For example, the built-up area of Delhi expanded from 373 km² in 1989 to 670 km² in 2011 (Mukhopadhyay *et al.*, 2013) and the population rose from 9.42 million in 1991 to 16.75 million in 2011 (Census, 2020). Consequently, the increase in fog frequency has been associated with increasing air pollution, in particular NO₂ concentrations (Jenamani, 2007). Additionally, poor visibility days (<4 km) in India have also been increasing in frequency, correlated with a decrease in wind speed and an increase in relative humidity (Jaswal *et al.*, 2013). In the Terai region, the southernmost region of Nepal bordering the Indo-Gangetic Plains (IGP) of India, the increase in fog frequency was found to be supported by a decrease in the daily maximum screen temperature (consistent with an increase in fogs that persist during the day), an increase in the daily minimum screen temperature (consistent with deep fogs slowing surface cooling; Price, 2011) and an increase in the screen level relative humidity (Shrestha *et al.*, 2018).

The large-scale circulation can also impact fog frequency (Syed *et al.*, 2012; Hingmire *et al.*, 2019). The North Atlantic Oscillation (NAO; Syed *et al.*, 2012) and Arctic Oscillation (AO; Hingmire *et al.*, 2019) have been found to relate to the interannual variability of fog frequency in the IGP. However, changes in the large-scale circulation were not found to be responsible for the fog frequency trend. Studies have identified a regime shift: a large increase in fog frequency seen in 1997/1998 accompanied by a decrease in temperature and visibility after 1997/1998 (Syed *et al.*, 2012; Kutty *et al.*, 2019; Gunturu and Kumar, 2021). The regime shift in fog frequency in the late 1990s has previously been associated with western disturbance (WD) activity (Gunturu and Kumar, 2021). Kutty *et al.* (2019) noted that the regime shift in fog frequency in 1998 coincided with a particularly strong El Niño year, potentially increasing the intensity of WDs (Dimri, 2013). Conversely, Gunturu and Kumar (2021) found a decrease in WD activity from 1996 to 1997 resulted in an increased frequency of clear skies leading to more surface radiative cooling and

consequently fog. In summary, no one factor has been identified that can fully explain the recent fog trend in India. Additional physical drivers, such as increased use of irrigation and changes in atmospheric aerosol loading from agriculture practices, for example, crop residue burning, continue to be proposed (Shrestha *et al.*, 2018; Kutty *et al.*, 2019). For the moment the main cause of the increasing fog trend remains an open question.

Previous studies describe scenarios where western disturbances—cyclonic circulations or troughs in the mid- and lower-troposphere that propagate eastward across northern India—lead to fog formation. WDs are typically associated with extreme wintertime rainfall in northern India (Dimri *et al.*, 2015). However, the Indian forecast manual also gives two example case studies where WDs can lead to fog in the IGP (Rao and Srinivasan, 1969). The first example of fog is in the rear of a WD, following its passage, where the conditions are ideal for fog formation: low winds, an increase in boundary-layer absolute humidity caused by rainfall from the WD and a cold stable boundary-layer. The second example is when fog forms ahead of a WD and such a WD centred over northern Pakistan results in light easterlies over northern India with a small increase in dew point temperature promoting fog formation. Conversely, WDs have also been associated with wintertime nonfoggy days (Hingmire *et al.*, 2019). Additionally, in Nepal no significant trend was observed in fog season rainfall, which is inferred to be dominated by WD events, despite the increase in foggy days (Shrestha *et al.*, 2018). Although these WD–fog relationships have been acknowledged as important by a range of studies (Syed *et al.*, 2012; Sawaisarje *et al.*, 2014; Dimri and Chevuturi, 2016; Ghude *et al.*, 2017; Hingmire *et al.*, 2019), none have sought to quantify the relationship between WDs and fog or present a thorough analysis of these events.

Fog is often classified by its formation mechanism and can be categorized into types, including: radiation, advection, cloud base lowering, evaporation and precipitation (Tardif and Rasmussen, 2007). In northern India studies have generally focused on radiation fog case studies (Syed *et al.*, 2012; Sathiyamoorthy *et al.*, 2016; Hingmire *et al.*, 2019; Pithani *et al.*, 2019a; Kutty *et al.*, 2021) with a few studies on advection fog (Pithani *et al.*, 2019b) but the relative frequencies of different fog types have not previously been examined. Categorizing fog events by their formation mechanism could help identify the crucial processes responsible for changes in fog frequency.

Our research aims to

- Present the first classification and climatology of different fog types in India.
- Quantify the proportion of fog events which are influenced by western disturbances.

- Improve understanding of the physical and synoptic relationships between western disturbances and fog.
- Thereby generate insight into the possible drivers behind the observed increasing trend in fog frequency in India.

The paper is structured as follows. In section 2 we describe the data used and the fog type classification algorithm. Section 3 presents and discusses the results of our India fog type classification, assesses the temporal trends of different fog types and examines the relationship between WDs and radiation fog events. This is followed by a discussion (section 4) and conclusions (section 5).

2 | DATA AND METHODS

2.1 | Observations

Three hourly meteorological data from 69 SYNOP sites in India have been examined over the period from January 2000 to January 2020 (Figure 1). There is >90% data available at each site over this study period. High and frequent data availability is necessary for the fog classification algorithm. Many sites prior to 2000 have lower data availability, in part due to the change from 6-hourly observations prior to 2000 to 3-hourly thereafter. Consequently, we cannot extend our study back as far as some other studies that use a “fog day” metric. These data were accessed from the Centre for Environmental Data Archive (CEDA) (MetOffice, 2012). For the analysis at Delhi it was possible to extend the study period to cover January 1993–January 2020 with a >90% data availability while at Lucknow and Patna it could be extended to cover January 1997–January 2020.

2.2 | Fog typology

An objective fog type classification algorithm (Tardif and Rasmussen, 2007) has been applied and adapted for many locations to understand the behaviour of fogs, for example, New York (Tardif and Rasmussen, 2007), Greece (Stolaki *et al.*, 2009), South Africa (Van Schalkwyk and Dyson, 2013), South Korea (Belorid *et al.*, 2015), Japan (Akimoto and Kusaka, 2015) and China (Gu *et al.*, 2019). The original algorithm used hourly data to ascertain the fog formation mechanism (Tardif and Rasmussen, 2007). However, it has been successfully adapted to be used with 3-hourly data (Belorid *et al.*, 2015). We further adapt the version for 3-hourly data as shown in Figure 2. The onset of fog is defined as

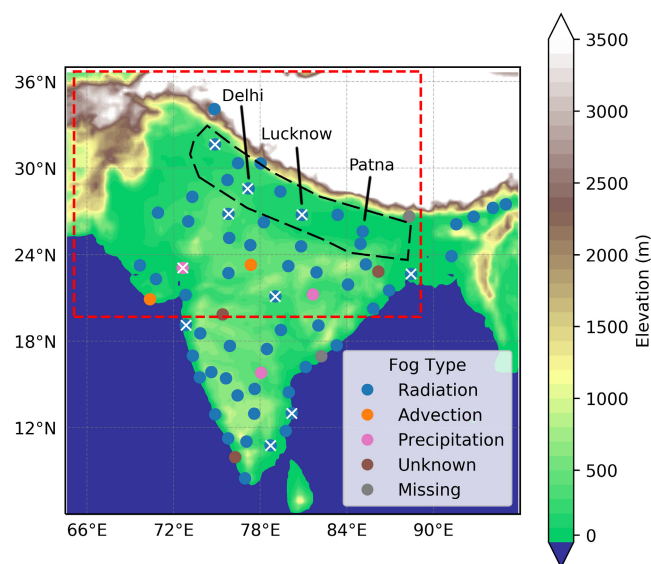


FIGURE 1 Surface elevation map of India with the location of SYNOP (circles) and METAR (crosses) where the colour of the circle shows the most common fog type. The black dashed line indicates the area known as the Indo-Gangetic Plains. The red box marks the area of the MODIS images shown in Figures 6 and 7 [Colour figure can be viewed at wileyonlinelibrary.com]

when the visibility first drops below 1 km and fog is reported in the present weather code. After a fog event is identified, it is classified by formation mechanism based on thresholds of several meteorological variables including visibility, air temperature, dew point temperature, wind speed, cloud cover and present weather. The algorithm classifies fog into five types, namely

- **Radiation fog (RAD):** It is formed by the overnight radiative cooling of the surface reducing the air's ability to hold moisture: the temperature drops to the dew point, thus water vapour begins to condense and fog droplets form. For an event to be classified as radiation fog it must meet all of the following criteria: wind speed at fog onset less than 2.5 m s^{-1} , cloud cover less than 25%, a cooling prior to fog onset or a cooling between 3 and 6 hr before onset and between sunset and sunrise.
- **Advection fog (ADV):** It is caused by the advection of warm moist air over a cold surface, cooling the air mass and reducing its ability to hold moisture. For an event to be classified as advection fog it must meet the following criteria: wind speed at fog onset more than 2.5 m s^{-1} and cloud cover less than 25%. Often studies define advection fog as a wall of fog reducing visibility suddenly and as such use an additional criteria in the algorithm which must be met, for example, visibility must drop from 8 to 1 km in the 9 hr prior to onset

(Belorid *et al.*, 2015). Here, we do not include this criteria due to the low background visibility in some regions in India (Jenamani, 2007).

- **Cloud base lowering fog (CBL):** It forms as the base of stratus clouds lower until they reach the surface. For an event to be classified as cloud base lowering fog, cloud cover must be greater than 25% and the cloud base higher than 1 km 6 hr prior to onset and lowering until onset.
- **Precipitation fog (PCP):** It forms by falling rain drops evaporating resulting in cooling and recondensation. The air is cooled until it reaches dew point and water vapour condenses out again. For an event to be classified as precipitation fog precipitation must be measured 3 hr prior to onset.
- **Evaporation fog (EVP):** It forms by cold air passing over a warmer and moister surface. The moisture from the warm surface evaporates into cold air with a lower saturation vapour pressure. The air above the surface warms causing it to rise and mix with the cold air above leading to supersaturation and activation of fog droplets. For an event to be classified as evaporation fog cloud cover must be below 25%, the rise in temperature lower than the rise in dew point temperature and onset should not occur between sunset and sunrise.

If the type cannot be classified using this algorithm then the fog events have been separated into two alternative types: “unknown” where the algorithm cannot categorize the fog type as none of the criteria are met and “missing” where the algorithm is unable to classify the fog type due to missing data prior to fog onset.

The fog type was classified based on three hourly observations, a lower temporal resolution than many previous studies (Tardif and Rasmussen, 2007; Stolaki *et al.*, 2009; Van Schalkwyk and Dyson, 2013; Akimoto and Kusaka, 2015; Gu *et al.*, 2019), which might affect fog classification. However, using three hourly data allowed us to significantly expand our study both in terms of the number of sites (69 instead of 10) and the length of the study period (from 2000 instead of 2012). We also performed tests to establish the reliability of using the 3-hourly version of the classification algorithm by using the smaller sample of data for 10 sites from 2012 to 2019 and using both the 3-hourly SYNOP data and hourly METAR data (Data S1, Supporting Information). The 3-hourly version compared well against the hourly version producing similar proportions of the different fog types. Note we also apply the algorithm to classify dense fog by changing the visibility threshold from 1 km to 200 m, the first step

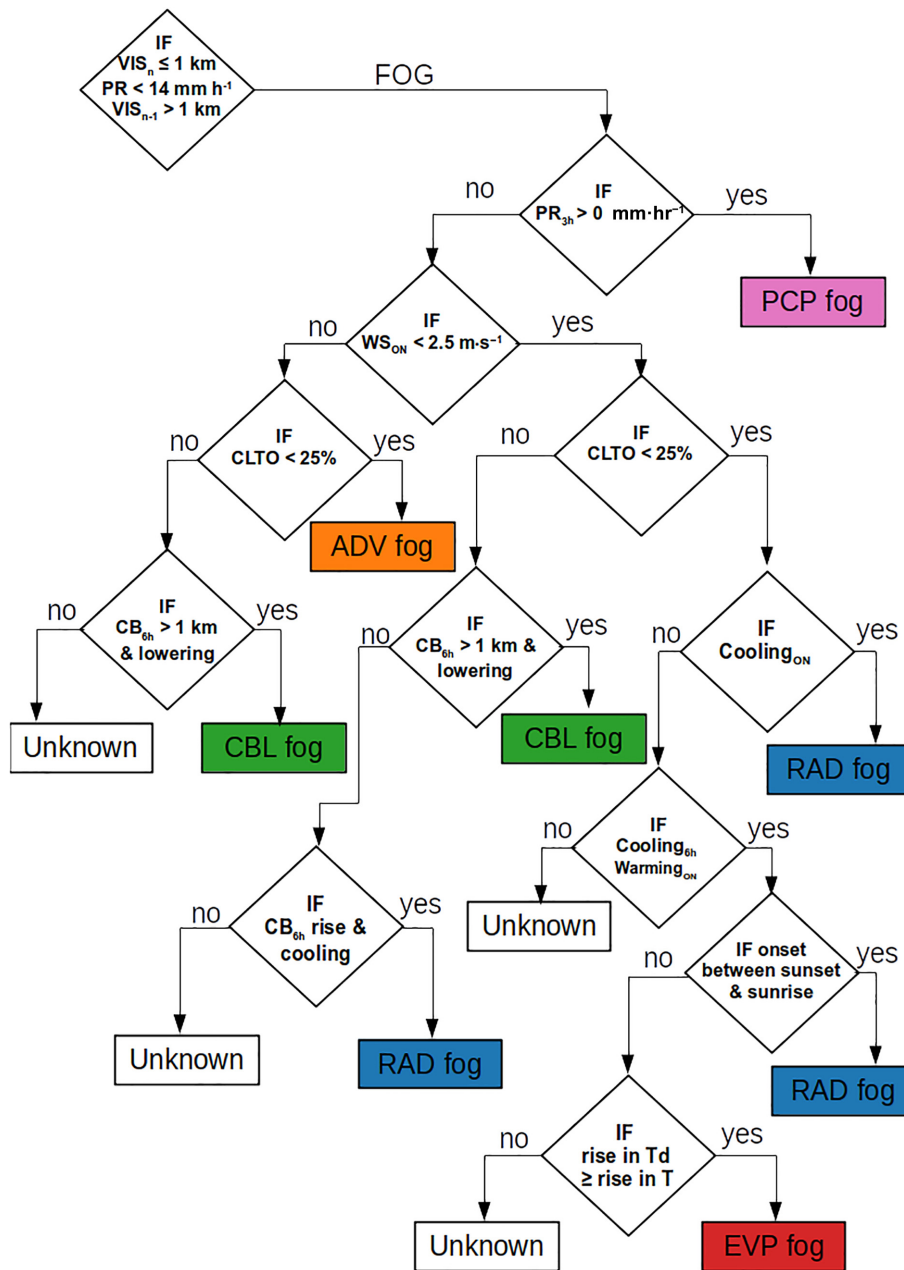


FIGURE 2 The fog classification algorithm adapted from Tardif and Rasmussen (2007) and Belorid *et al.* (2015). T and Td refer to screen air temperature and dew point temperature, respectively. WS is 10 m wind speed. CLTO is total cloud cover and CB is cloud base height. Subscript ON is at the time of fog onset, 3 hr/6 hr are 3/6 hr prior to fog onset. n is the time of potential onset and $n - 1$ is the previous observation time. See text for fog type definitions [Colour figure can be viewed at [wileyonlinelibrary.com](https://onlinelibrary.wiley.com/doi/10.1002/joc.7832)]

depicted in Figure 2. See section 3.1 for the justification of this adaptation. In section 3.1 we present annual data. To investigate the trends in fog events and the relationship to WDs (in section 3.2 onwards) we focus on results based on December and January which are the months the majority of WDs (Hunt *et al.*, 2018) and fog occur (Srivastava *et al.*, 2016).

2.3 | Western disturbance tracks

We use a western disturbance tracks dataset (Hunt *et al.*, 2018) to quantify the link between WDs and radiation fog. The WD tracks dataset covers 1979–

2015. We use from 1993 to 2015 to coincide with Delhi SYNOP data. Western disturbances are detected by a tracking algorithm applied to ERA-I reanalysis data (Dee *et al.*, 2011). The tracking algorithm detects WDs based on upper-level (450–300 mb) vorticity maxima and groups points within 1,000 km during consecutive time steps to form tracks. The tracks are then filtered to ensure they are consistent with the definition of a WD. First, they are filtered by length—a track must persist for 2 days. Second, tracks must pass through Pakistan or northern India, defined as the region 20°–36.5°N, 60°–80°E. Finally tracks must propagate eastward. See Hunt *et al.* (2018) for further details.

2.4 | ERA-5

ERA-5 reanalysis data are used in section 3.3.3 to produce spatial composite plots of key atmospheric variables for fog events relating to different WD clusters. In section 3.3.3, anomalies are calculated as the difference from the December January mean from 1992 to 2019. ERA-5 is a global reanalysis dataset produced using the European Centre for Medium-range Weather Forecasts (ECMWF) Integrated Forecast System (IFS) with a horizontal resolution of 31 km (see Hersbach *et al.*, 2020 for details).

2.5 | MODIS True Color images

We use the Moderate Resolution Imaging Spectroradiometer (MODIS) corrected reflectance (True Color) product from NASA's Terra satellite. The product uses reflectance of visible wavelengths leaving the top of the atmosphere, centred at 645 nm (red), 555 nm (green), and 469 nm (blue) to produce the True Color images. These images are used to illustrate WD and fog events in section 3.3. Images were extracted from <https://worldview.earthdata.nasa.gov>.

3 | RESULTS

3.1 | Fog typology

The classification algorithm identifies a total of 10,262 fog events at 69 SYNOP sites from 2000 to 2020 for all months. The algorithm reproduces the spatial distribution of the annual frequency of fog events seen in previous studies which have been based upon reports of fog days (Syed *et al.*, 2012; Srivastava *et al.*, 2016). The highest number of fog events occurs in the Indo-Gangetic plains (IGP) region in the north with an average of 54 events per year at Delhi, 45 events per year at Patna and 39 events per year at Lucknow. The number of fog events differs from studies that use fog *days* as here fog lasting for multiple days is only counted as a single event. In southern India fog events are rare with less than three events per year observed at most sites with the exception of a few coastal locations.

Considering the 69 station network as a whole, the proportion of different fog types is radiation 68.1%, precipitation 6.8%, evaporation 3.2%, advection 3.0% and cloud base lowering 2.4%; with 11.1% unidentified due to not meeting the algorithm criteria, primarily when the cooling rate is $0 \text{ K}\cdot\text{hr}^{-1}$ prior to fog onset, and 5.4% unidentified when data is missing (Figure 3). Radiation fog is the dominant fog type at 59 out of 69 stations

(Figure 1), even in some coastal regions which typically have a greater chance of advection fog events (Tardif and Rasmussen, 2007). For comparison, radiation fog accounted for 38.5% of all fog events in Korea (Belorid *et al.*, 2015), 51.2% at the Cape Town International Airport in South Africa (Van Schalkwyk and Dyson, 2013) and almost half in Japan (Akimoto and Kusaka, 2015). In New York state precipitation fog was most frequent accounting for 36% of all events, followed by radiation fog accounting for 28% (Tardif and Rasmussen, 2007). Comparing the fog type frequency in India to these other locations highlights the prevalence of radiation fog and this is partially explained by the very low mean wind speeds over northern India in December and January (Jaswal and Koppa, 2013).

In the IGP region the background visibility is generally low in December and January with the visibility rarely above 5,000 m (Jenamani, 2007; Singh and Dey, 2012; Tyagi *et al.*, 2017; Kutty *et al.*, 2019). Jenamani (2007) found that between 1999 and 2003 the visibility was above 5,000 m for only 0.3 hr per day in December and 0 hr per day in January. Using the 1 km visibility threshold for identifying fog onset, the accompanying maximum relative humidity (RH) of the event ranged from 70 to 100% and only on 70% of occasions was the RH above 95% (Figure 4). The other 30% of cases may be considered as haze events with visibility reduced due to high aerosol concentrations despite the criteria used in the algorithm. Previous studies in India suggest that a threshold of 200 m is a better indication of the presence of fog (Ghude *et al.*, 2017; Pithani *et al.*, 2020). This lower threshold also corresponds to cases where the low visibility has a high impact. For both of these reasons we also implemented the fog typology algorithm using a 200 m threshold. The maximum RH is above 95% for 84% of these dense fog cases confirming that this threshold is more appropriate for indicating fog onset in the IGP region. However, there are still 16% of cases when the maximum RH is below 95% which could be defined as dense haze. The number of cases with the RH below 95% indicates the importance of dry and hydrated aerosol concentrations for visibility reduction in India. Indeed, hydrated aerosol can cause up to 68% of the light scattering in fog (Hammer *et al.*, 2014; Elias *et al.*, 2015) with this proportion potentially increasing in India where the aerosol concentrations are larger (Ghude *et al.*, 2017). Delhi and Lucknow experienced the highest frequency of dense fog events, 24 events per year. Changing the visibility threshold has little impact on the types of fog observed in India with radiation fog still the dominant type occurring in 70.0% of dense fog events (Figure 3) and the dominant fog type at 59 of the 69 sites. Given the dominance of radiation fog in India we do not examine the spatial variance of the different fog types further.

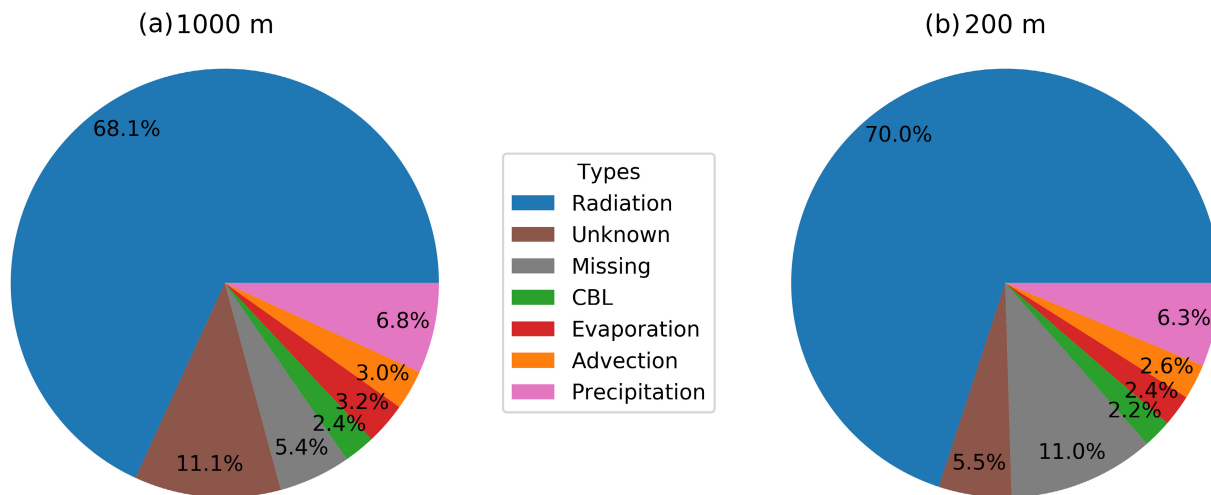


FIGURE 3 Fog type proportions using (a) the 1,000 m visibility threshold (10,262 events in total) and (b) 200 m visibility threshold (6,123 events in total) at all stations between 2000 and 2020 [Colour figure can be viewed at wileyonlinelibrary.com]

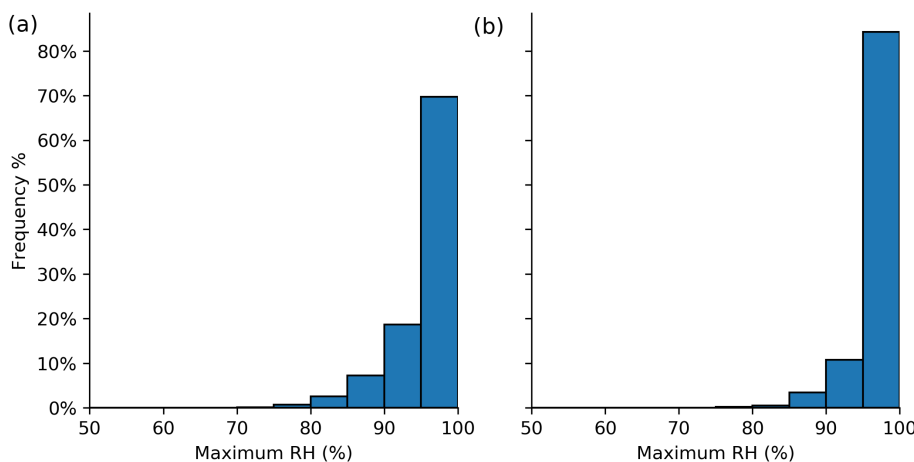


FIGURE 4 The maximum relative humidity during an event using the 1,000 m (a) and 200 m (b) visibility thresholds at all stations between 2000 and 2020 [Colour figure can be viewed at wileyonlinelibrary.com]

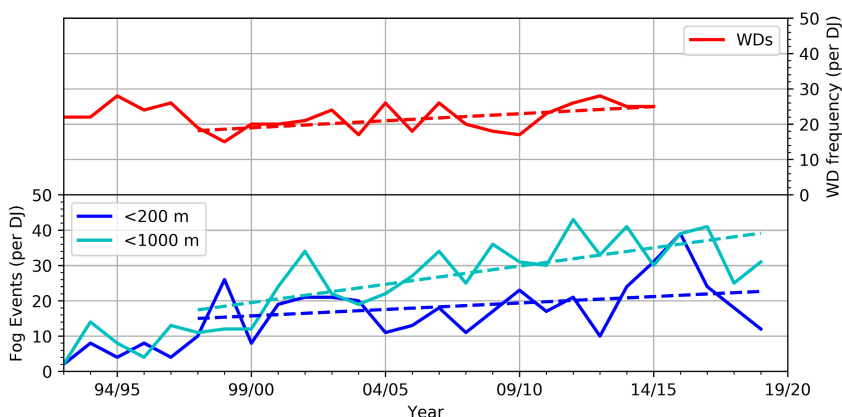


FIGURE 5 Number of fog (cyan) and dense fog (blue) events which occur each winter (December and January) at Delhi. Number of western disturbance (WD) events (red) each winter which pass within a 1,000 km of Delhi. Linear regression lines starting in 1997/1998 are overlaid (dashed lines) [Colour figure can be viewed at wileyonlinelibrary.com]

3.2 | December and January trends

Figure 5 shows the frequency of fog events (vis <1,000 m) and dense fog events (vis <200 m) per year in December and January (DJ) at Delhi. Recall, an event is defined as a continuous period when the visibility is

below the respective threshold, thus a fog event can last several days and contain multiple dense fog events. Previous studies have found a distinct step change in visibility in 1997/1998 (Syed *et al.*, 2012; Kutty *et al.*, 2019) and given this, and the data available, we focus on the trend from 1997/1998. There is a statistically significant

TABLE 1 Frequency (%) and trend (change in the number events per year per DJ) for each fog type from 1997/1998 to 2018/2019 at selected locations for both fog and dense fog events

Site	RAD	ADV	CBL	PCP	EVP	ALL	RH \geq 95%
Delhi, 1 km	70.2% (0.77)	6.2% (0.12)	1.9% (–)	2.4% (–)	4.7% (0.05)	619 (1.03)	411 (1.21)
Delhi, 200 m	68.1% (0.18)	3.6% (–)	2.6% (–)	2.9% (–)	7.0% (0.11)	413 (0.36)	353 (0.51)
Lucknow, 1 km	70.2% (0.95)	3.8% (–)	2.2% (–)	3.9% (–)	3.2% (–)	584 (1.26)	395 (0.44)
Lucknow, 200 m	77.1% (0.81)	2.7% (–)	1.5% (–)	3.1% (–)	2.2% (–)	406 (0.88)	363 (0.74)
Patna, 1 km	66.4% (0.87)	1.7% (–)	0.9% (–)	1.9% (–)	1.6% (–)	734 (0.85)	473 (0.72)
Patna, 200 m	73.7% (0.42)	2.6% (–)	0.8% (–)	2.6% (–)	0.1% (–)	342 (0.59)	308 (0.56)

Note: The ALL column contains the total number of events and the trend regardless of type. The RH \geq 95% column shows number of events when the maximum RH is over 95% and the trend (change in the number events per year per DJ) regardless of type. The bold values indicate statistical significance at $p < .05$. Trends are not shown if the average number of events per year is less than 1. The unknown and missing types are not shown.

increase, $p < .05$, in the frequency of fog events and a statistically nonsignificant increasing trend in the frequency of dense fog events (Table 1).

The frequency of each fog type at Delhi is similar to the proportion of each fog type for all sites (Table 1 and Figure 3). The greatest difference is seen for evaporation (dense) fog events at Delhi which occur in 4.7% (7.0%) compared to the total proportion for all sites, 2.8% (2.5%). There are statistically significant positive trends at Delhi for the fog events regardless of type (1.03 events per DJ), radiation fog (0.77 events per DJ) and the advection fog events (0.12 events per DJ). For dense fog events and other fog types the trends are insignificant.

At Lucknow and Patna there are statistically significant positive trends in the number of fog events regardless of type (1.26 and 0.85 events per DJ, respectively) and for radiation fog specifically (0.81 and 0.87 events per DJ, respectively). Unlike over Delhi, there is also statistically significant positive trend in the number of dense fog events at Lucknow and Patna (0.88 and 0.59 events per DJ, respectively).

Additionally, we examine events when the maximum RH is \geq 95% to remove events that could be defined as haze events. In general, we find similar trends to those based on all humidity conditions. At Delhi, we find a larger increasing trend when including the additional threshold requiring maximum RH to be \geq 95%, 1.21 rather than 1.03 events per DJ, when using the 1 km threshold. This suggests that the direct reduction in visibility caused by suspended particles in the atmosphere makes a small contribution to the observed increasing trend in low visibility events. However, the magnitudes of these trends using the \geq 95% RH threshold are smaller than for all RH conditions and for all visibility thresholds at Lucknow and Patna. The only change in statistical significance is at Lucknow where the increasing trend, using the 1 km threshold, is reduced to a statistically insignificant 0.44 events per DJ from a statistically

significant 1.26 events per DJ. This smaller increasing trend at Lucknow and Patna, when RH \geq 95%, suggests that the direct reduction in visibility caused by suspended particles in the atmosphere (i.e., haze events) makes an important contribution to the overall observed increasing trend in low visibility events but is not the only cause.

Radiation fog has the most significant role due to its relative frequency compared to the other types. The relationship between WDs and radiation fog and the consequences this relationship may have on the observed fog frequency trend is explored now. A discussion of other contributing drivers of the fog frequency trend is contained in section 4.

3.3 | Western disturbances and radiation fog

Figures 6 and 7 illustrate two example WD-fog scenarios; one for each of the two types described by Rao and Srinivasan (1969) are selected as they show fog when the satellite pass occurs at 1030 local time when fog has often dissipated. Figure 6 shows a WD passing over northern India producing precipitation over the region on the 17th and 18th January 2013 followed by rising pressure. The resulting clear skies and low wind speeds combined with the additional surface and near-surface moisture provided by precipitation from the WD create the ideal conditions for radiation fog formation meeting all the criteria in the fog typology algorithm. The presence of widespread fog is clearly visible in the MODIS image. Meanwhile, Figure 7 shows a WD over Jammu and Kashmir on the 24th and 25th January 2009. On the 24th there is widespread fog over Bihar, east Uttar Pradesh and the Terai region of Nepal. On the 25th as the WD develops and precipitation increases, the winds change to a light easterly and some of the cloud dissipates over Uttar Pradesh and Delhi. The low wind speeds and clear skies

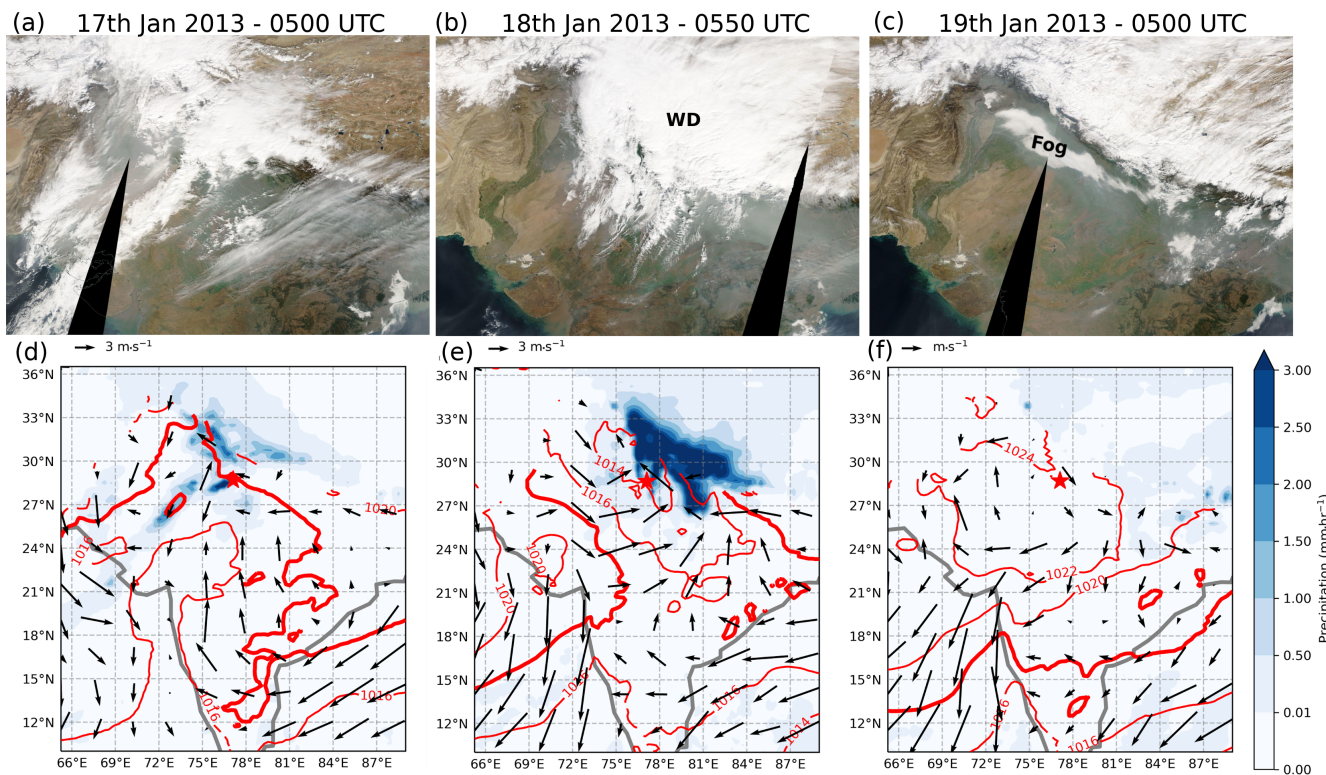


FIGURE 6 A western disturbance propagating over northern India resulting in widespread fog. The top row shows MODIS imagery indicating the presence of a western disturbance on (a) the 17th January 2013 at 0500 UTC and (b) 18th January 2013 at 0550 UTC and (c) fog on the 19th January 2013 at 0500 UTC. The bottom row shows ERA5 sea level pressure at 2 mb spacing, the thick contour highlights the 1,018 mb isobar (mb, red contour), 10 m winds (black vectors) and precipitation rate ($\text{mm}\cdot\text{hr}^{-1}$, blue shading) on (d) the 17th at 0500 UTC, (e) 18th at 0600 UTC, (f) and 19th at 0500 UTC January 2013 [Colour figure can be viewed at wileyonlinelibrary.com]

allow for sufficient surface cooling and radiation fog to form further west, again meeting all the criteria in the fog typology algorithm for radiation fog. The fog spreads northwestwards leading to a widespread fog impacting Uttar Pradesh and Delhi.

We use a WD track dataset (Hunt *et al.*, 2018) to quantify the link between WDs and (dense) radiation fog over Delhi, Lucknow and Patna. To examine the relationship between fog and dense fog with WDs the following criteria were applied to the fog events identified using the classification algorithm:

- Only radiation fog cases selected—the most common fog type.
- Only cases in December or January were selected—the months with the peak number of fog events and western disturbances.

The composite WD analysis by Hunt *et al.* (2018) uses a distance of 1,000 km from the centre of WDs to examine their structure. They determine this distance through an examination of 19 published cases. We use the same

distance, 1,000 km, to determine if a WD is influencing the meteorology over Delhi at fog onset. Five hundred and twenty WD tracks pass within 1,000 km of Delhi in December and January between 1992/1993 and 2014/2015. Using the above criteria WDs influence 46.9% of both radiation fog (168 events) and dense radiation fog events (105 events) at Delhi. WDs influence a smaller percentage of events at Lucknow and Patna, 30.4 and 22.1%, respectively, for radiation fog events and 37.4 and 21.6%, respectively, for dense radiation fog events between 1997/1998 and 2014/2015 (Table 2). Conversely (20.2%) 32.3% of WDs which are within 1,000 km of Delhi coincide with a (dense) fog event. Although WDs are important in terms of the number of radiation fog events which coincide with WDs there is still a large proportion (68–80%) of WDs which do not coincide with a fog event. Understanding the properties of WDs which do not coincide with fog events is important but beyond the scope of this research. Using Welch's *t* test, as we have unequal sample sizes, the onset time and duration of fog events are found to be independent of any association with a WD suggesting that, although WDs may provide a

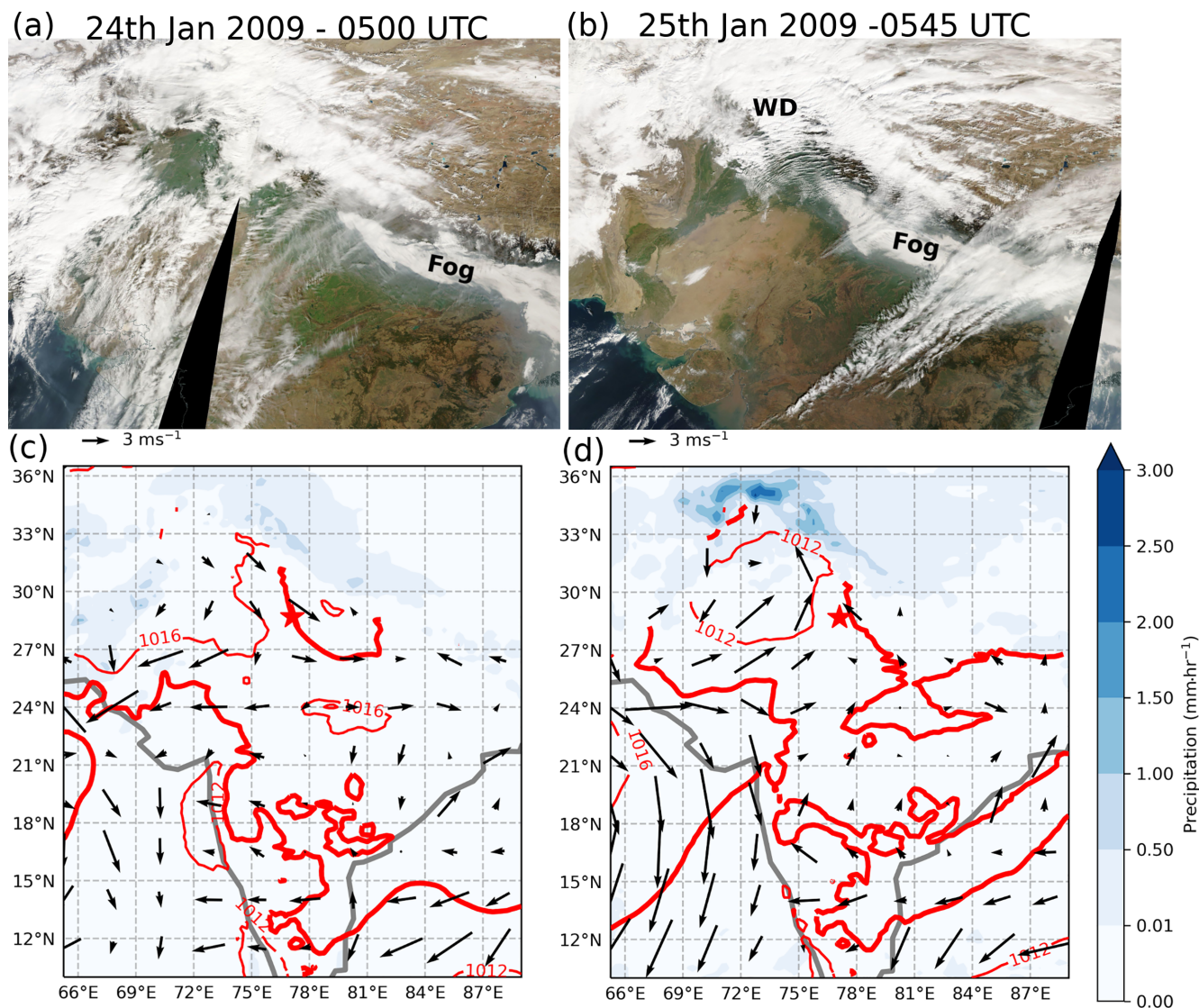


FIGURE 7 A western disturbance over the northwest of India resulting in the expansion of a widespread fog. The top row shows MODIS imagery indicating the presence of a western disturbance and fog on (a) the 24th at 0500 UTC and (b) 25th January 2009 at 0545 UTC. The bottom row shows ERA5 sea level pressure at 2 mb spacing, the thick contour highlights the 1,014 mb isobar (mb, red contour), 10 m winds (black vectors) and precipitation rate ($\text{mm}\cdot\text{hr}^{-1}$, blue shading) on (c) the 24th and (d) 25th January 2009 [Colour figure can be viewed at wileyonlinelibrary.com]

favourable environment for fog formation, they do not significantly influence its life-cycle.

3.3.1 | December and January trends

Similar to fog events there has also been a statistically significant increase (0.40 events per DJ, $p < .05$) in the number of WDs which propagate within 1,000 km of Delhi between 1997/1998 and 2014/2015 (Figure 5). Here, we investigate the correlation between the number of (dense) fog events and WDs (Table 2). There is a positive correlation between the number of WDs and (dense)

fog events at all three sites (Table 2) with the exception of Delhi where there is a weak negative correlation between the number of WDs and dense fog events.

Generally, there is a statistically significant increase in the frequency of (dense) radiation fogs both with and without an associated WD. However, there are statistically insignificant trends in dense fog events at Delhi, in radiation fog events at Patna without the influence of a WD and dense radiation fog events at Patna in the presence of a WD. As both the (dense) radiation fogs with or without an associated WD have increasing trends, WDs cannot be considered the primary driver for the observed increasing frequency of fog events.

TABLE 2 The Pearson correlation coefficient between the number of WDs and number of radiation fog events and the total number of radiation fog events, from 1997/1998 to 2014/2015, associated or not with WDs with the trend in brackets (events per year in December and January).

Site	Pearson's r	WD-fog	No WD-fog
Delhi, 1 km	0.52	163 (0.56)	180 (0.55)
Delhi, 200 m	-0.08	101 (0.16)	119 (-0.01)
Lucknow, 1 km	0.34	93 (0.39)	212 (0.70)
Lucknow, 200 m	0.35	85 (0.45)	142 (0.49)
Patna, 1 km	0.26	81 (0.31)	286 (0.63)
Patna, 200 m	0.30	44 (0.09)	160 (0.65)

Note: The bold values indicate a statistical significance of $p < .05$.

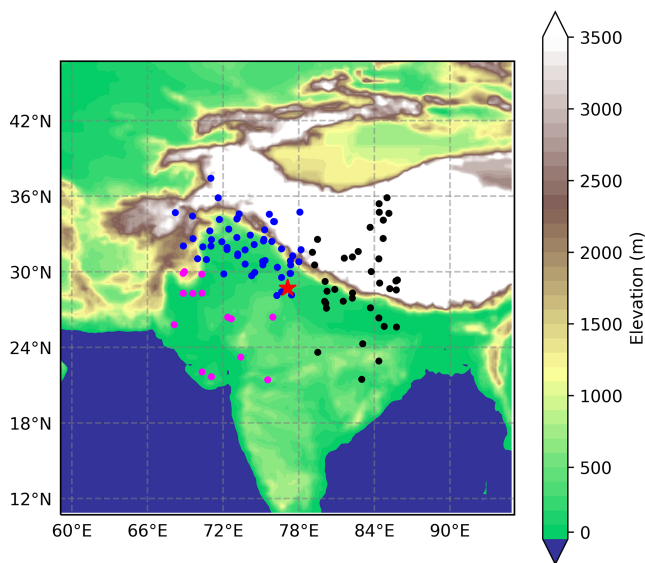


FIGURE 8 The position of WDs at fog onset. The red star marks the Delhi site. Coloured dots are the clusters identified by the K -means clustering, to the northwest (blue), southwest (magenta) and east (black) of Delhi [Colour figure can be viewed at [wileyonlinelibrary.com](https://onlinelibrary.wiley.com)]

3.3.2 | Western disturbance position

The 105 dense radiation fog events related to WDs at Delhi have been categorized into three types dependent on WD position at dense fog onset using K -means clustering (Figure 8). The optimal number of types was determined using the “elbow” method (Kodinariya and Makwana, 2013) in the scikit-learn python package (Pedregosa *et al.*, 2011). The three K -means clustering types fit to three positions in relation to Delhi, to the northwest for 54 cases (51.4% of cases), southwest for 14 cases (13.3% of cases) and east for 37 cases (35.2% of cases). The east cluster appears to correspond well with the position of a WD with fog forming in the rear

(e.g., Figure 6) and the northwest cluster appears to correspond well with the position of a WD with fog forming ahead of the WD (e.g., Figure 7), that is, the two examples in the forecasting manual (Rao and Srinivasan, 1969). The southwest cluster is the rarest and has not previously been described. An examination of the WD position at Lucknow and Patna broadly adhere to the findings at Delhi.

3.3.3 | Composite structure at the onset of dense radiation fog

By using composites of the three positional WD clusters and comparing these to mean conditions in December–January we investigate the processes which contribute to dense fog formation. The composites presented are masked where orographic height is over 2,000 m. The dense fog event composite without the influence of WDs shows a positive pressure anomaly with a peak of 1.25 mb over the north of India (Figure 9a). Positive pressure anomalies are typical for radiation fog formation and are consistent with the mean sea level pressure anomaly composites previously demonstrated for widespread fog days in Hingmire *et al.* (2019). Conversely, the northwest WD composite (Figure 9b) has a generally weak negative pressure anomaly, consistent with the case shown in Figure 7 and typical of WDs positioned over the northwest with a low pressure anomaly to the east of the track centre (Hunt *et al.*, 2018). Similarly, the southwest WD composite has a negative pressure anomaly (Figure 9c). The east WD composite has a more pronounced positive pressure anomaly south of Delhi (Figure 9d) which is consistent with WDs positioned to the east of Delhi and with the example shown in Figure 6 with a positive pressure anomaly positioned to the west of the WD track centre (Hunt *et al.*, 2018).

All of the dense fog composites are colder at 950 mb than the January and December average (Figure 10). The peak cold anomaly differs in detail between composites. Without the presence of a WD (Figure 10a) the cold anomaly peak is in the southeast of the domain, approximately 3 K colder than average. The northwest WD composite appears similar but with the cold peak further west and marginally less cold (Figure 10b). Both the southwest and east composites have a similar temperature pattern to each other with a colder peak further west and closer to Delhi (Figure 10c,d). The peak cold anomaly in the southwest and east composites is stronger than the peak for the no WD and the northwest composites, approximately 4 K colder than average.

At the onset of a dense fog event without the presence of a WD there is a positive specific humidity anomaly to

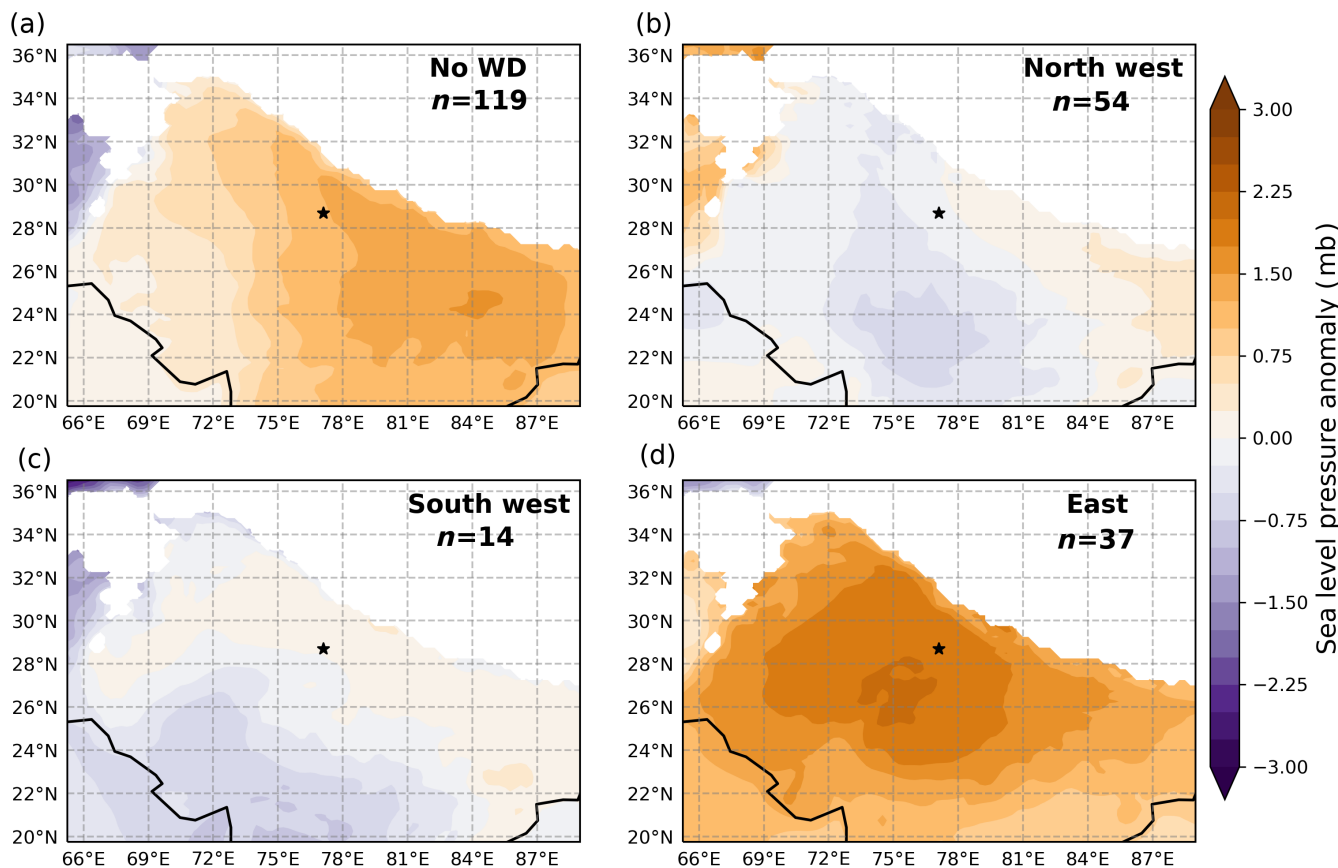


FIGURE 9 Sea level pressure anomaly (mb) at dense fog onset relative to the December and January mean for the dense fog cases (a) not influenced by WDs, (b) northwest WD cluster, (c) southwest WD cluster and (d) east WD cluster. The black star marks Delhi. The white area masks data where the orography is over 2,000 m [Colour figure can be viewed at [wileyonlinelibrary.com](https://onlinelibrary.wiley.com/doi/10.1002/joc.7832)]

the northwest, approximately $1 \text{ g}\cdot\text{kg}^{-1}$ moister than average over Delhi itself (Figure 11a). The northwest WD composite also has a generally higher than the average specific humidity, again approximately $1 \text{ g}\cdot\text{kg}^{-1}$ moister than average over Delhi (Figure 11b). The southwest and east composites have a smaller positive specific humidity anomaly, typically within $0.5 \text{ g}\cdot\text{kg}^{-1}$ of the average (Figure 11c,d). In short, all dense fog composites are moister than average in the Delhi region.

The wind speeds over the Indo-Gangetic Plains are lower than average in the composite without the presence of a WD and in the northwest and southwest composites, by around $1 \text{ m}\cdot\text{s}^{-1}$ (Figure 12). We find 36.3% of the northwest cluster cases have near-surface easterly winds over Delhi, such as those in Figure 7, which corresponds to the previous description of fog forming ahead of a WD (Rao and Srinivasan, 1969). The remaining cases have either northerly or westerly winds. The east composite winds are consistent with Figure 6 with slightly higher ($<1 \text{ m}\cdot\text{s}^{-1}$) than average northwesterly winds over Delhi but lower than average wind speeds to the northwest of Delhi.

In summary, a number of typical characteristics have been highlighted regarding the synoptic environment in

which fog forms in the Delhi region. Fog formation can occur in a higher than average surface pressure environment without the presence of WDs but can also occur ahead of and to the rear of a WD. The key features at fog onset with or without the presence of a WD are a slightly colder, moister atmosphere with lower than average wind speeds, meeting the criteria for radiation fog formation (see section 2.2). However, the presence and positioning of the WD impacts the spatial extent of these favourable conditions.

4 | DISCUSSION

The observed upward trend in fog frequency is dominated by the radiation fog type (Table 1). The results here suggest that the positive trend in WD frequency is not the main cause of the observed upward trend in fog frequency; the frequency of (dense) radiation fogs increases both with and without an associated WD. There is a positive correlation between the frequency of fog events and the number of WDs per December and January but there is not a correlation between the number of WDs and the

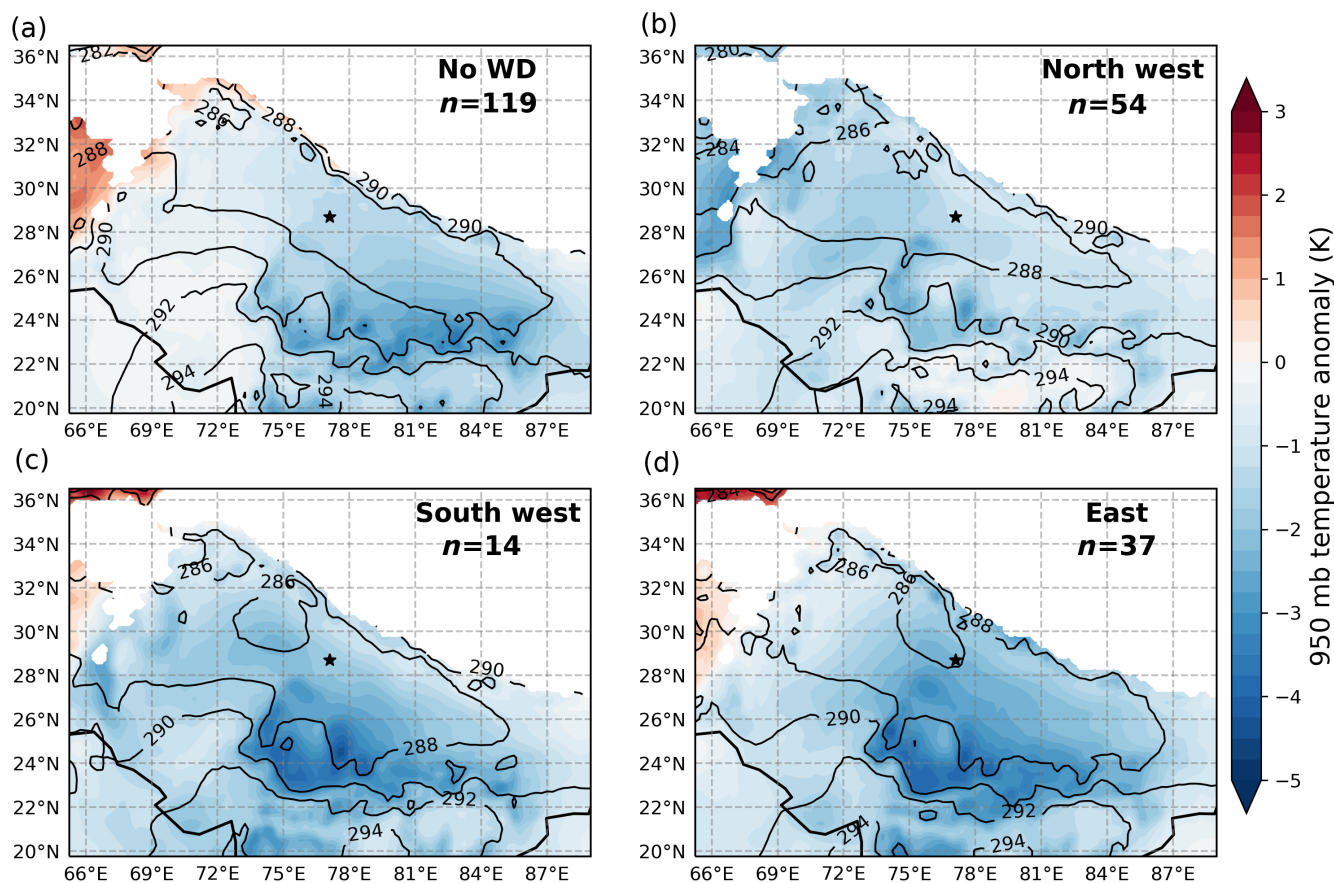


FIGURE 10 950 mb temperature anomaly (K) at dense fog onset relative to the January and December mean 950 mb temperature for the dense fog cases (a) not influenced by WDs, (b) northwest WD cluster, (c) southwest WD cluster and (d) east WD cluster. Black contours are the mean 950 mb temperature (K) at fog onset. The black star marks Delhi. The white area masks data where the orography is over 2,000 m [Colour figure can be viewed at [wileyonlinelibrary.com](https://onlinelibrary.wiley.com/doi/10.1002/joc.7832)]

number of dense fog events at Delhi, suggesting WDs are not responsible for the interannual variability of dense fog events either. However, there could be a relationship between dense fog frequency and the number of WDs with specific properties, for example precipitation rate and average WD track position, which should be investigated in future work. We have quantified and examined the features of WDs which lead to fog formation; however, contrasting these WDs to those 70–80% which do not lead to fog could provide vital guidance for forecasters in fog prediction. Categorizing WDs by their intensity, precipitation or dynamic features (such as Hunt *et al.*, 2018) and assessing whether these features determine whether a WD will lead (or not lead) to fog should be investigated in the future. Rainfall amount and/or intensity also varies from one WD event to another. The case by case impact of WDs on the likelihood of fog formation will also depend in detail on antecedent catchment conditions and the local capacity of the heterogeneous land surface to enable infiltration in each case. The timing of a WD passage may also be important

in terms of supporting or acting against normal diurnal processes. We have shown that fog in the IGP can occur in a range of synoptic environments all of which need to be forecast realistically in order to accurately reproduce these fog events and as such future work should include an assessment of the synoptic scale as well as the local drivers of fog events, for example, radiative cooling, turbulence, surface processes and aerosol–fog interactions.

We have utilized a WD climatology based on a tracking algorithm (Hunt *et al.*, 2018). Other studies have based the relationship between WDs and fog on the assumption that wintertime rainfall is predominantly caused by WDs (Shrestha *et al.*, 2018; Gunturu and Kumar, 2021). However, not all WDs lead to precipitation and thus the definition and detection of WDs can differ between studies (Hunt *et al.*, 2018). Indeed, Midhuna *et al.* (2020) found that the number of WDs in daily weather reports did not correspond well with the western disturbance index derived from the NCEP reanalysis dataset using the 850 and 200 mb geopotential height difference, a finding they attributed to the daily reports only

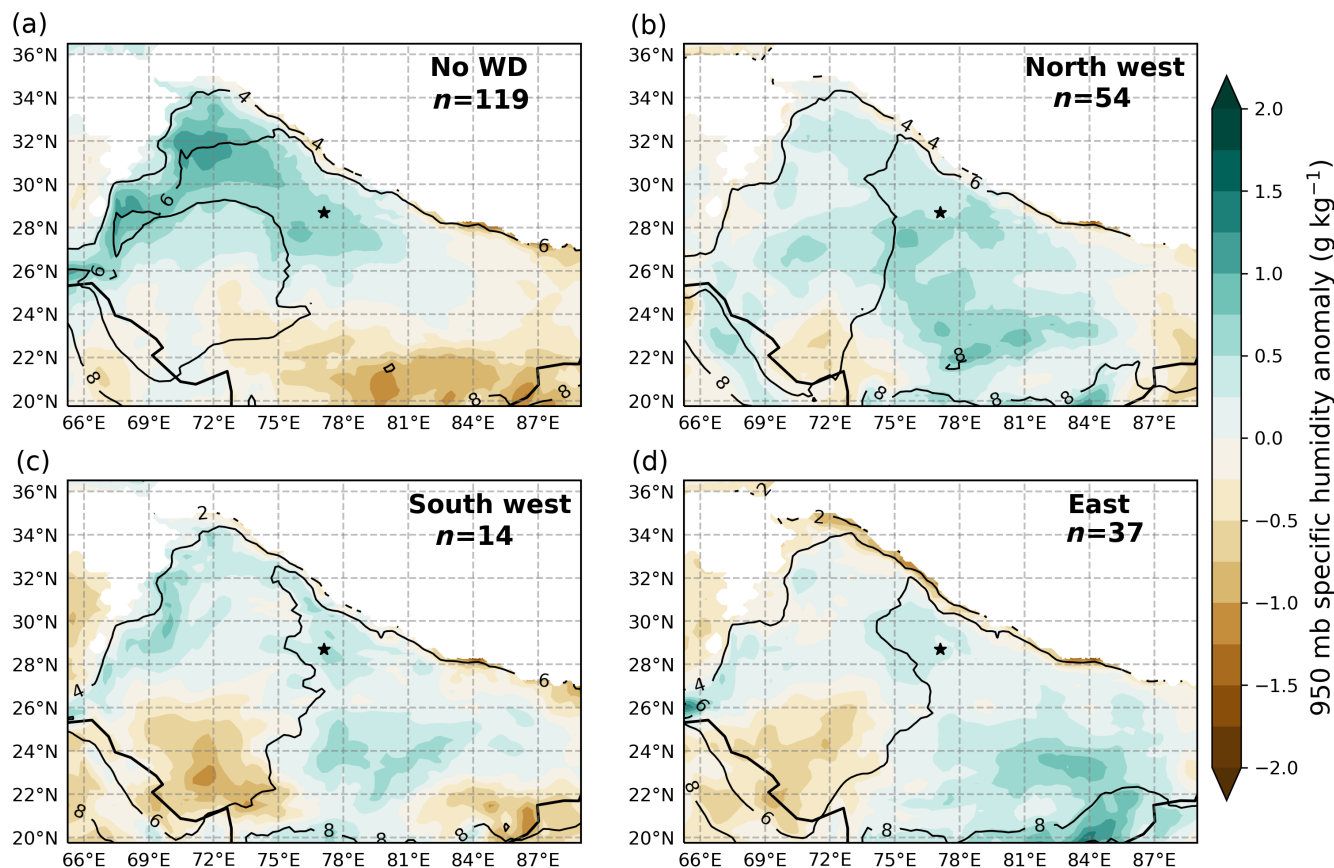


FIGURE 11 950 mb specific humidity ($\text{g}\cdot\text{kg}^{-1}$) anomaly at dense fog onset relative to the January and December mean 950 mb specific humidity for the dense fog cases (a) not influenced by WDs, (b) northwest WD cluster, (c) southwest WD cluster and (d) east WD cluster. Black contours are the mean 950 mb specific humidity (K) at fog onset. The black star marks Delhi. The white area masks data where the orography is over 2,000 m [Colour figure can be viewed at [wileyonlinelibrary.com](https://onlinelibrary.wiley.com)]

recording precipitating WDs. These definition differences could impact relationships found between fog and WDs. Other approaches could be employed to determine relationships between weather type and fog such as using weather patterns (Neal *et al.*, 2020) or satellite derived fog datasets (Egli *et al.*, 2019).

Our results imply that drivers other than WD frequency, such as changes in local and regional aerosol pollution, are likely the primary driver responsible for the observed trend in fog frequency, directly or indirectly. Many cities in India, for example Delhi, are rapidly expanding. Increasing population and urban expansion has led to greater air pollution emissions, vehicle and biomass sources being particular issues in the winter focus season (Sharma and Dikshit, 2016; Jain *et al.*, 2018; 2020) and additional contributions from diesel generator sets, industry, waste burning and from brick kilns close to Delhi (Guttikunda and Calori, 2013). These emissions have resulted in increasing concentrations of NO_x and particulate matter in Delhi (Gurjar *et al.*, 2016) with the highest concentrations of particulate matter observed in November, December and January (Anand *et al.*, 2019;

Molina, 2021). Consequently, Indian cities have some of the highest $\text{PM}_{2.5}$ concentrations in the world (Molina, 2021).

Aerosol changes can have several impacts on visibility and fog frequency. First, increasing near-surface aerosol concentrations can directly reduce visibility. We show that the visibility reduction caused directly by aerosol makes an important contribution to the increasing trend in low visibility events. Second, increasing aerosol concentration modifies fog microphysics and thus the visibility reduction caused by fogs. Third, the absorption and scattering of solar radiation caused by aerosols can modify near-surface temperature and humidity changing the frequency of fog events. In Delhi increasing NO_2 concentrations have previously been correlated with increased fog frequency (Jenamani, 2007). Indeed, the decrease (increase) of fog in urban areas has been suggested to correlate with decreases (increases) in emissions of NO_x and SO_2 as these are precursors for small, hygroscopic particles (Klemm and Lin, 2016). However, there is a complex relationship between expanding urban land use, increasing aerosol concentrations and fog frequency. A change in

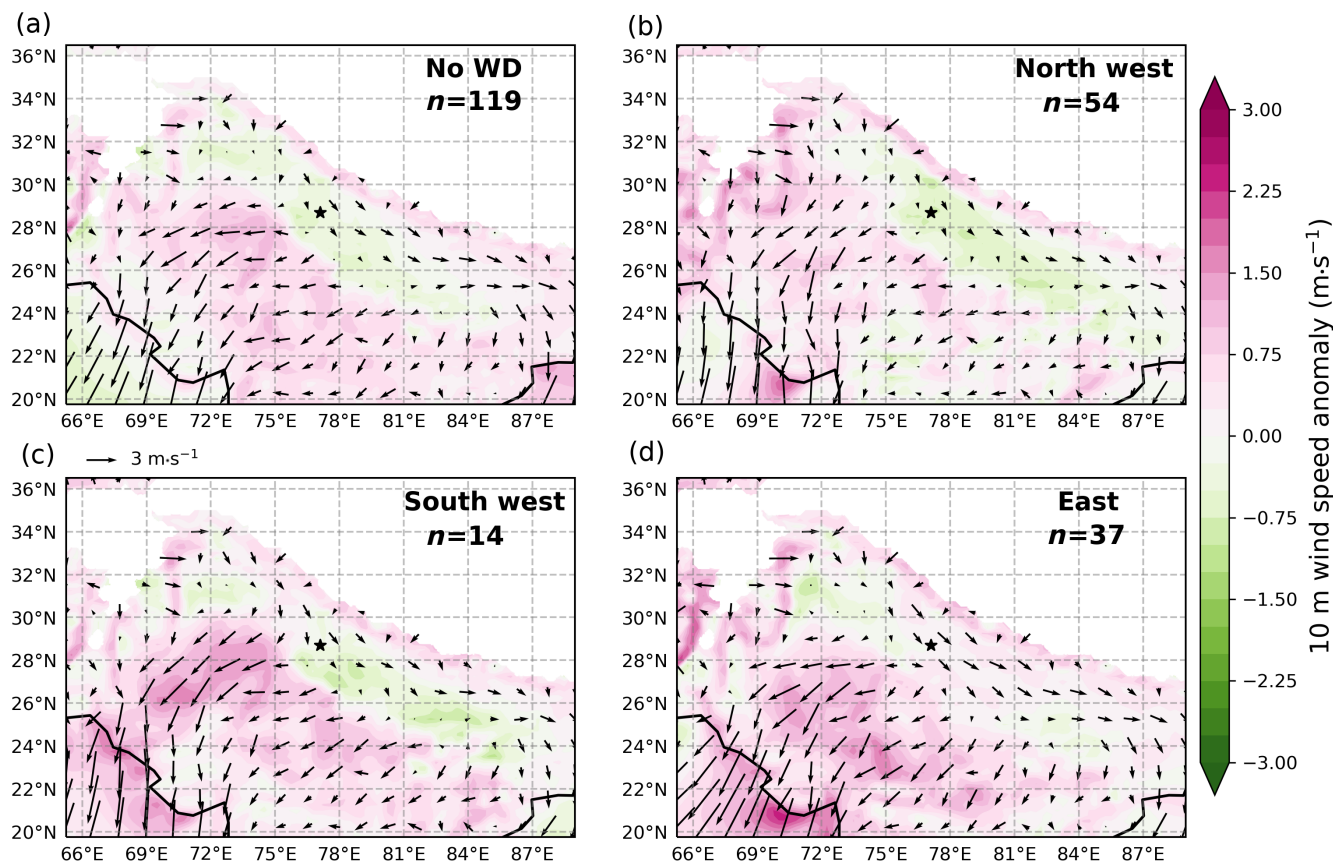


FIGURE 12 10 m wind speed anomaly at dense fog onset relative to the January and December mean 10 m wind speed for the dense fog cases (a) not influenced by WDs, (b) northwest WD cluster, (c) southwest WD cluster and (d) east WD cluster. The vectors show the mean wind speed and direction at fog onset. The black star marks Delhi. The white area masks data where the orography is over 2,000 m [Colour figure can be viewed at [wileyonlinelibrary.com](https://onlinelibrary.wiley.com)]

temperature of 0.1°C has the same effect on visibility as a 10% change in aerosol concentration during a fog event (Klemm and Lin, 2016). The competing effects of the urban heat island and aerosol concentrations on fog frequency have been explored in other urban areas where the observed fog frequency trend is decreasing (Yan *et al.*, 2020). In these locations the urban heat island effect dominates the aerosol impacts causing the decrease in fog frequency (Yan *et al.*, 2020). Although an increase in aerosol typically increases liquid water content (LWC) and fog droplet number (Stolaki *et al.*, 2015; Maalick *et al.*, 2016; Poku *et al.*, 2019), aerosol (cloud condensation nuclei) concentrations can reach a critical concentration that suppresses fog due to water vapour competition, resulting in a lower LWC and droplet number (Yan *et al.*, 2020). Further research is needed to determine whether aerosol concentrations over Delhi have reached this critical concentration. If Delhi is in the aerosol repressed regime then this could explain the cause of the insignificant increasing trend in dense fog frequency and weak correlations between WDs and dense fog compared to the significant trends at the other sites examined.

Aerosols can indirectly impact on fog frequency via a feedback on the radiation balance rather than directly by decreasing visibility or impacting the microphysical properties of fog (Bott, 1991). Aerosol optical depth is dependent on the synoptic conditions in the IGP (Kaskaoutis *et al.*, 2014). An increase in aerosol optical depth has been shown to contribute to a warming, between 950 and 800 mb, in east China and consequently a weakening of the East Asian winter monsoon providing more favourable conditions for fog (Niu *et al.*, 2010). Indeed, despite the increase in wintertime aerosol optical depth over Delhi and northern India (Babu *et al.*, 2013; Mehta, 2015; Srivastava, 2017) there is also evidence of the urban heat island effect punching holes into widespread fog events over the IGP (Gautam and Singh, 2018). The complex interaction between WDs, the urban heat island effect and aerosol concentration will be the focus of our future research. In particular, the development of numerical weather prediction models for this region with its dependence upon realistic aerosol characteristics and parameterisations (Dey, 2018). Additionally, the development of city scale models is also key for the improvement of fog

forecasts in India (Boutle *et al.*, 2016; Jayakumar *et al.*, 2018; Smith *et al.*, 2021).

5 | CONCLUSIONS

We identified 10,262 fog events at 69 SYNOP sites across India over 20 years. Using a 1 km visibility threshold to identify fog onset, 30% of events had a maximum relative humidity of less than 95% highlighting the frequency that visibility is reduced to below 1 km by aerosols alone. Radiation fog has previously been stated to be the most common fog type in India (Syed *et al.*, 2012; Sathiyamoorthy *et al.*, 2016; Hingmire *et al.*, 2019; Pithani *et al.*, 2019a). We have used an objective fog type classification algorithm for the first time over India to quantify the radiation fog contribution as representing 68.1 and 70.0% of <1 km and <200 m fog events, respectively. This represents a very high share compared to other locations around the world, due to the very low mean wind speeds over northern India in December and January (Jaswal and Koppa, 2013).

Previous studies have highlighted the importance of WDs for the presence of fog in the IGP. For the first time, we quantify the proportion of radiation fog and dense radiation fog events over Delhi associated with WDs as 46.9 and 46.9%, respectively. We categorize the WDs associated with dense radiation fog into 3 types, according to their position at fog onset. Two of these three types correspond well to the previous descriptions of WD fog scenarios (Rao and Srinivasan, 1969): the northwest cluster (fog forming ahead of the WD) and the east cluster (fog forming in the rear of the WD) which occur in 51.4 and 35.2% of fog events associated with WDs, respectively. Additionally, our analysis identified a third previously unidentified positional type of WD coincident with fog, positioned to the southwest. The southwest cluster occur infrequently with only 14 occurring in the 22 years examined, resulting in subtle but supportive changes to the atmosphere which lead to fog. The subtlety of the changes and the infrequent occurrence of these events is likely to be the reason that these have not previously been identified. Through the generation of composite patterns of surface variables, our research has highlighted robust and distinctive anomalies associated with different western disturbance types, providing a valuable reference point in support of operational fog forecasting (Rao and Srinivasan, 1969). Meanwhile successfully distinguishing between fog types helps focus the forecasting task either on local or regional processes, as appropriate.

We have found an increasing trend in radiation fog frequency both associated with and without WDs. Therefore, although we have shown WDs can provide the conditions for fog formation, trends in the frequency of WD

events cannot account for the observed fog frequency trends. We postulate that the increasing frequency of fog events is instead a result of a complex interaction between urban expansion and the associated changes in aerosol loading both locally and transported from other regions. Considering that urban expansion increases the impact of the urban heat island effect reducing fog, our hypothesis is that the primary driver for the increasing fog frequency trend is the increased aerosol concentrations. However, the precise aerosol process that leads to the change in fog frequency needs further investigation with impacts on the surface radiation balance, the direct reduction in visibility from the absorption and scattering of visible light by aerosol and the indirect aerosol effect on fog microphysics all likely playing a role.

In summary, we have highlighted the importance of radiation fog in India and presented its occurrence in various synoptic environments. With the increasing trend in the frequency of these fog events in India and the impact they have on travel, winter crop production and consequently food security their prediction urgently needs to be improved through targeted enhancements to forecasting systems.

ACKNOWLEDGEMENTS

This work was funded through the Weather and Climate Science for Service Partnership (WCSSP) India, a collaborative initiative between the Met Office, supported by the UK Government's Newton Fund, and the Indian Ministry of Earth Sciences (MoES). The authors would like to acknowledge all the helpful comments at the WCSSP India meetings during the development of this work. We would like to thank the three anonymous reviewers for their constructive comments that have improved our manuscript.

DATA AVAILABILITY STATEMENT

The SYNOP data are available from the Centre for Environmental Data Archive (CEDA; <http://catalogue.ceda.ac.uk/uuid/220a65615218d5c9cc9e4785a3234bd0>). The ERA-5 reanalysis data were downloaded from the Copernicus Climate Change Service (C3S) Climate Data Store (<https://climate.copernicus.eu/climate-reanalysis>). The Western Disturbance tracks dataset is available from the Centre for Environmental Data Archive (CEDA; <https://catalogue.ceda.ac.uk/uuid/233cf64c54e946e0bb691a07970ec245>). The MODIS images were extracted from <https://worldview.earthdata.nasa.gov>.

ORCID

Daniel K. E. Smith  <https://orcid.org/0000-0003-0818-672X>

Ian A. Renfrew  <https://orcid.org/0000-0001-9379-8215>

REFERENCES

- Akimoto, Y. and Kusaka, H. (2015) A climatological study of fog in Japan based on event data. *Atmospheric Research*, 151, 200–211.
- Anand, V., Korhale, N., Rathod, A. and Beig, G. (2019) On processes controlling fine particulate matters in four Indian megacities. *Environmental Pollution*, 254, 113026.
- Ashley, W.S., Strader, S., Dziubla, D.C. and Habberlie, A. (2015) Driving blind: weather-related vision hazards and fatal motor vehicle crashes. *Bulletin of the American Meteorological Society*, 96, 755–778.
- Babu, S.S., Manoj, M.R., Moorthy, K.K., Gogoi, M.M., Nair, V.S., Kompalli, S.K., Satheesh, S.K., Niranjan, K., Ramagopal, K., Bhuyan, P.K. and Singh, D. (2013) Trends in aerosol optical depth over Indian region: potential causes and impact indicators. *Journal of Geophysical Research: Atmospheres*, 118, 11794–11806.
- Belorid, M., Lee, C.B., Kim, J.C. and Cheon, T.H. (2015) Distribution and long-term trends in various fog types over South Korea. *Theoretical and Applied Climatology*, 122, 699–710.
- Bott, A. (1991) On the influence of the physico-chemical properties of aerosols on the life cycle of radiation fogs. *Boundary-Layer Meteorology*, 56, 1–31.
- Boutle, I.A., Finnenkoetter, A., Lock, A.P. and Wells, H. (2016) The London model: forecasting fog at 333 m resolution. *Quarterly Journal of the Royal Meteorological Society*, 142, 360–371.
- Census. (2020) *Delhi population 2011–2020 census*. Available at: <https://www.census2011.co.in/census/state/delhi.html>.
- Dee, D.P., Uppala, S.M., Simmons, A.J., Berrisford, P., Poli, P., Kobayashi, S., Andrae, U., Balmaseda, M.A., Balsamo, G., Bauer, P., Bechtold, P., Beljaars, A.C.M., van de Berg, L., Bidlot, J., Bormann, N., Delsol, C., Dragani, R., Fuentes, M., Geer, A.J., Haimberger, L., Healy, S.B., Hersbach, H., Hólm, E. V., Isaksen, I., Kållberg, P., Köhler, M., Matricardi, M., McNally, A.P., Monge-Sanz, B.M., Morcrette, J.-J., Park, B.-K., Peubey, C., de Rosnay, P., Tavolato, C., Thépaut, J.-N. and Vitart, F. (2011) The ERA-Interim reanalysis: configuration and performance of the data assimilation system. *Quarterly Journal of the Royal Meteorological Society*, 137, 553–597.
- Dey, S. (2018) On the theoretical aspects of improved fog detection and prediction in India. *Atmospheric Research*, 202, 77–80.
- Dimri, A. (2013) Relationship between enso phases with northwest India winter precipitation. *International Journal of Climatology*, 33, 1917–1923.
- Dimri, A.P. and Chevuturi, A. (2016) *Western Disturbances—An Indian Meteorological Perspective*. New York, NY: Springer.
- Dimri, A.P., Niyogi, D., Barros, A.P., Ridley, J., Mohanty, U.C., Yasunari, T. and Sikka, D.R. (2015) Western disturbances: a review. *Reviews of Geophysics*, 53, 225–246.
- Egli, S., Thies, B. and Bendix, J. (2019) A spatially explicit and temporally highly resolved analysis of variations in fog occurrence over Europe. *Quarterly Journal of the Royal Meteorological Society*, 145, 1721–1740.
- Elias, T., Dupont, J.-C., Hammer, E., Hoyle, C.R., Haeffelin, M., Burnet, F. and Jolivet, D. (2015) Enhanced extinction of visible radiation due to hydrated aerosols in mist and fog. *Atmospheric Chemistry and Physics*, 15, 6605–6623.
- Gautam, R. and Singh, M.K. (2018) Urban Heat Island over Delhi punches holes in widespread fog in the Indo-Gangetic Plains. *Geophysical Research Letters*, 45, 1114–1121.
- Ghude, S.D., Bhat, G.S., Prabhakaran, T., Jenamani, R.K., Chate, D. M., Safai, P.D., Karipot, A.K., Konwar, M., Pithani, P., Sinha, V., Rao, P.S.P., Dixit, S.A., Tiwari, S., Todekar, K., Varpe, S., Srivastava, A.K., Bisht, D.S., Murugavel, P., Ali, K., Mina, U., Dharua, M., Rao, J., Padmakumari, B., Hazra, A., Nigam, N., Shende, U., Lal, D.M., Chandra, B.P., Mishra, A.K., Kumar, A., Hakkim, H., Pawar, H., Acharja, P., Kulkarni, R., Subharthi, C., Balaji, B., Varghese, M., Bera, S. and Rajeevan, M. (2017) Winter fog experiment over the Indo-Gangetic plains of India. *Current Science*, 112, 767.
- Gonçalves, F.L.T., da Rocha, R.P., Fernandes, G.P. and Petto, S., Jr. (2008) Drizzle and fog analysis in the São Paulo metropolitan area: changes 1933–2005 and correlations with other climate factors. *Die Erde*, 139, 61–76.
- Gu, Y., Kusaka, H., Doan, V.Q. and Tan, J. (2019) Impacts of urban expansion on fog types in Shanghai, China: numerical experiments by WRF model. *Atmospheric Research*, 220, 57–74.
- Gultepe, I., Sharman, R., Williams, P.D., Zhou, B., Ellrod, G., Minnis, P., Trier, S., Griffin, S., Yum, S.S., Gharabaghi, B., Feltz, W., Temimi, M., Pu, Z., Storer, L.N., Kneringer, P., Weston, M.J., Chuang, H.Y., Thobois, L., Dimri, A.P., Dietz, S. J., França, G.B. and Almeida, M.V. (2019) A review of high impact weather for aviation meteorology. *Pure and Applied Geophysics*, 176, 1869–1921.
- Gunturu, U.B. and Kumar, V. (2021) Weakened baroclinic activity causes an abrupt rise in fog in the indo-gangetic plain. *Geophysical Research Letters*, 48, e2021GL096114.
- Gurjar, B., Ravindra, K. and Nagpure, A.J. (2016) Air pollution trends over Indian megacities and their local-to-global implications. *Atmospheric Environment*, 142, 475–495.
- Guttikunda, S.K. and Calori, G. (2013) A GIS based emissions inventory at 1 km × 1 km spatial resolution for air pollution analysis in Delhi, India. *Atmospheric Environment*, 67, 101–111.
- Hameed, S., Mirza, M.I., Ghauri, B.M., Siddiqui, Z.R., Javed, R., Khan, A.R., Rattigan, O.V., Qureshi, S. and Husain, L. (2000) On the widespread winter fog in northeastern Pakistan and India. *Geophysical Research Letters*, 27, 1891–1894.
- Hammer, E., Gysel, M., Roberts, G.C., Elias, T., Hofer, J., Hoyle, C. R., Bukowiecki, N., Dupont, J.-C., Burnet, F., Baltensperger, U. and Weingartner, E. (2014) Size-dependent particle activation properties in fog during the ParisFog 2012/13 field campaign. *Atmospheric Chemistry and Physics*, 14, 10517–10533.
- Hersbach, H., Bell, B., Berrisford, P., Hirahara, S., Horányi, A., Muñoz-Sabater, J., Nicolas, J., Peubey, C., Radu, R., Schepers, D., Simmons, A., Soci, C., Abdalla, S., Abellan, X., Balsamo, G., Bechtold, P., Biavati, G., Bidlot, J., Bonavita, M., De Chiara, G., Dahlgren, P., Dee, D., Diamantakis, M., Dragani, R., Flemming, J., Forbes, R., Fuentes, M., Geer, A., Haimberger, L., Healy, S., Hogan, R.J., Hólm, E., Janisková, M., Keeley, S., Laloyaux, P., Lopez, P., Lupu, C., Radnoti, G., de Rosnay, P., Rozum, I., Vamborg, F., Villaume, S. and Thépaut, J.-N. (2020) The ERA5 global reanalysis. *Quarterly Journal of the Royal Meteorological Society*, 146, 1999–2049.
- Hingmire, D., Vellore, R.K., Krishnan, R., Ashtikar, N.V., Singh, B. B., Sabade, S. and Madhura, R.K. (2019) Widespread fog over the Indo-Gangetic Plains and possible links to boreal winter teleconnections. *Climate Dynamics*, 52, 5477–5506.
- Hunt, K.M.R., Turner, A.G. and Shaffrey, L.C. (2018) The evolution, seasonality and impacts of western disturbances. *Quarterly Journal of the Royal Meteorological Society*, 144, 278–290.

- Jain, S., Sharma, S., Vijayan, N. and Mandal, T. (2020) Seasonal characteristics of aerosols (PM_{2.5} and PM₁₀) and their source apportionment using PMF: a four year study over Delhi, India. *Environmental Pollution*, 262, 114337.
- Jain, S., Sharma, S.K., Mandal, T.K. and Saxena, M. (2018) Source apportionment of PM₁₀ in Delhi, India using PCA/APCS, UNMIX and PMF. *Particuology*, 37, 107–118.
- Jaswal, A. and Koppar, A. (2013) Climatology and trends in near-surface wind speed over India during 1961–2008. *Mausam*, 64, 417–436.
- Jaswal, A.K., Kumar, N., Prasad, A.K. and Kafatos, M. (2013) Decline in horizontal surface visibility over India (1961–2008) and its association with meteorological variables. *Natural Hazards*, 68, 929–954.
- Jayakumar, A., Rajagopal, E.N., Boutle, I.A., George, J.P., Mohandas, S., Webster, S. and Aditi, S. (2018) An operational fog prediction system for Delhi using the 330 m unified model. *Atmospheric Science Letters*, 19, e796.
- Jenamani, R.K. (2007) Alarming rise in fog and pollution causing a fall in maximum temperature over Delhi. *Current Science*, 93, 314–322.
- Jenamani, R.K. (2012) Development of intensity based fog climatological information system (daily and hourly) at IGI airport, New Delhi for use in fog forecasting and aviation. *Mausam*, 63, 89–112.
- Kapoor, P. (2019) Over 10,000 lives lost in fog-related road crashes. *Times of India*. Available at: <https://timesofindia.indiatimes.com/india/over-10000-lives-lost-in-fog-related-road-crashes/articleshow/67391588.cms> [Accessed on September 19, 2019].
- Kaskaoutis, D., Houssos, E., Goto, D., Bartzokas, A., Nastos, P., Sinha, P., Kharol, S.K., Kosmopoulos, P., Singh, R.P. and Takemura, T. (2014) Synoptic weather conditions and aerosol episodes over Indo-Gangetic Plains, India. *Climate Dynamics*, 43, 2313–2331.
- Klemm, O. and Lin, N. (2016) What causes observed fog trends: air quality or climate change. *Aerosol and Air Quality Research*, 16, 1131–1142.
- Kodinariya, T.M. and Makwana, P.R. (2013) Review on determining number of cluster in K-means clustering. *International Journal of Advance Research in Computer Science and Management Studies*, 1, 90–95.
- Kulkarni, R., Jenamani, R.K., Pithani, P., Konwar, M., Nigam, N. and Ghude, S.D. (2019) Loss to aviation economy due to winter fog in New Delhi during the winter of 2011–2016. *Atmosphere*, 10, 198.
- Kutty, S.G., Dimri, A.P. and Gultepe, I. (2019) Climatic trends in fog occurrence over the Indo-Gangetic plains. *International Journal of Climatology*, 40, 2048–2061.
- Kutty, S.G., Dimri, A.P. and Gultepe, I. (2021) Physical processes affecting radiation fog based on WRF simulations and validation. *Pure and Applied Geophysics*, 178, 4265–4288.
- Maalick, Z., Kühn, T., Korhonen, H., Kokkola, H., Laaksonen, A. and Romakkaniemi, S. (2016) Effect of aerosol concentration and absorbing aerosol on the radiation fog life cycle. *Atmospheric Environment*, 133, 26–33.
- Mehta, M. (2015) A study of aerosol optical depth variations over the Indian region using thirteen years (2001–2013) of MODIS and MISR Level 3 data. *Atmospheric Environment*, 109, 161–170.
- MetOffice. (2012) Met Office Integrated Data Archive System (MIDAS) Land and Marine Surface Stations Data (1853-current). NCAS British Atmospheric Data Centre. Available at: <http://catalogue.ceda.ac.uk/uuid/220a65615218d5c9cc9e4785a3234bd0>.
- Midhuna, T., Kumar, P. and Dimri, A. (2020) A new Western Disturbance Index for the Indian winter monsoon. *Journal of Earth System Science*, 129, 59.
- Molina, L.T. (2021) Introductory lecture: air quality in megacities. *Faraday Discussions*, 226, 9–52.
- Mukhopadhyay, A., Mukherjee, S., Garg, R. and Ghosh, T. (2013) Spatio-temporal analysis of land use-land cover changes in Delhi using remote sensing and GIS techniques. *International Journal of Geomatics and Geosciences*, 4, 213–223.
- Neal, R., Robbins, J., Dankers, R., Mitra, A., Jayakumar, A., Rajagopal, E.N. and Adamson, G. (2020) Deriving optimal weather pattern definitions for the representation of precipitation variability over India. *International Journal of Climatology*, 40, 342–360.
- Niu, F., Li, Z., Li, C., Lee, K.H. and Wang, M. (2010) Increase of wintertime fog in China: potential impacts of weakening of the eastern Asian monsoon circulation and increasing aerosol loading. *Journal of Geophysical Research: Atmospheres*, 115, D00K20.
- Pedregosa, F., Varoquaux, G., Gramfort, A., Michel, V., Thirion, B., Grisel, O., Blondel, M., Prettenhofer, P., Weiss, R., Dubourg, V., Vanderplas, J., Passos, A., Cournapeau, D., Brucher, M., Perrot, M. and Duchesnay, E. (2011) Scikit-learn: machine learning in python. *Journal of Machine Learning Research*, 12, 2825–2830.
- Pithani, P., Ghude, S.D., Chennu, V.N., Kulkarni, R.G., Steeneveld, G., Sharma, A., Prabhakaran, T., Chate, D.M., Gultepe, I., Jenamani, R.K. and Rajeevan, M. (2019a) WRF model prediction of a dense fog event occurred during the winter fog experiment (WIFEX). *Pure and Applied Geophysics*, 176, 1827–1846.
- Pithani, P., Ghude, S.D., Jenamani, R.K., Biswas, M., Naidu, C.V., Debnath, S., Kulkarni, R., Dhangar, N.G., Jena, C., Hazra, A., Phani, R., Mukhopadhyay, P., Prabhakaran, T., Nanjundiah, R. S. and Rajeevan, M. (2020) Real-time forecast of dense fog events over Delhi: the performance of the WRF model during the WIFEX field campaign. *Weather and Forecasting*, 35, 739–756.
- Pithani, P., Ghude, S.D., Prabhakaran, T., Karipot, A., Hazra, A., Kulkarni, R., Chowdhuri, S., Resmi, E.A., Konwar, M., Murugavel, P., Safai, P.D., Chate, D.M., Tiwari, Y., Jenamani, R.K. and Rajeevan, M. (2019b) WRF model sensitivity to choice of PBL and microphysics parameterization for an advection fog event at Barkachha, rural site in the Indo-Gangetic basin, India. *Theoretical and Applied Climatology*, 136, 1099–1113.
- Poku, C., Ross, A.N., Blyth, A.M., Hill, A.A. and Price, J.D. (2019) How important are aerosol–fog interactions for the successful modelling of nocturnal radiation fog? *Weather*, 74, 237–243.
- Price, J. (2011) Radiation fog. Part I: observations of stability and drop size distributions. *Boundary-Layer Meteorology*, 139, 167–191.
- Rao, Y.P. and Srinivasan, V. (1969) Discussion of Typical Synoptic Weather Situations: Winter - Western Disturbances and their associated features. *Forecasting Manual Part III*, pp. 31–33. Pune, India: Indian Meteorological Department.
- Sathiyamoorthy, V., Arya, R. and Kishtawal, C.M. (2016) Radiative characteristics of fog over the Indo-Gangetic Plains during northern winter. *Climate Dynamics*, 47, 1793–1806.

- Sawaisarje, G.K., Khare, P., Shirke, C.Y., Deepakumar, S. and Narkhede, N.M. (2014) Study of winter fog over Indian subcontinent: climatological perspectives. *Mausam*, 65, 19–28.
- Sharma, M. and Dikshit, O. (2016) Comprehensive study on air pollution and green house gases (GHGs) in Delhi. Final Report, Prepared by IIT Kanpur, sponsored by Delhi Pollution Control Committee, New Delhi, p. 289.
- Shrestha, S., Moore, G.A. and Peel, M.C. (2018) Trends in winter fog events in the Terai region of Nepal. *Agricultural and Forest Meteorology*, 259, 118–130.
- Singh, A. and Dey, S. (2012) Influence of aerosol composition on visibility in megacity Delhi. *Atmospheric Environment*, 62, 367–373.
- Singh, S. and Singh, D. (2010) Recent fog trends and its impact on wheat productivity in NW plains in India. In: *5th International Conference on Fog*. Münster, Germany: Fog Collection and Dew Münster, pp. 25–30.
- Smith, D.K.E., Renfrew, I.A., Dorling, S.R., Price, J.D. and Boutle, I. A. (2021) Sub-km scale numerical weather prediction model simulations of radiation fog. *Quarterly Journal of the Royal Meteorological Society*, 147, 746–763.
- Srivastava, R. (2017) Trends in aerosol optical properties over South Asia. *International Journal of Climatology*, 37, 371–380.
- Srivastava, S.K., Sharma, A.R. and Sachdeva, K. (2016) A ground observation based climatology of winter fog: study over the Indo-Gangetic Plains, India. *International Journal of Environmental, Chemical, Ecological, Geological and Geophysical Engineering*, 10, 705–716.
- Srivastava, S.K., Sharma, A.R. and Sachdeva, K. (2017) An observation-based climatology and forecasts of winter fog in Ghaziabad, India. *Weather*, 72, 16–22.
- Stolaki, S., Haefelin, M., Lac, C., Dupont, J.-C., Elias, T. and Masson, V. (2015) Influence of aerosols on the life cycle of a radiation fog event. A numerical and observational study. *Atmospheric Research*, 151, 146–161.
- Stolaki, S.N., Kazadzis, S.A., Foris, D.V. and Karacostas, T.S. (2009) Fog characteristics at the airport of Thessaloniki, Greece. *Natural Hazards and Earth System Sciences*, 9, 1541–1549.
- Sugimoto, S., Sato, T. and Nakamura, K. (2013) Effects of synoptic-scale control on long-term declining trends of summer fog frequency over the Pacific side of Hokkaido Island. *Journal of Applied Meteorology and Climatology*, 52, 2226–2242.
- Syed, F.S., Körnich, H. and Tjernström, M. (2012) On the fog variability over South Asia. *Climate Dynamics*, 39, 2993–3005.
- Tardif, R. and Rasmussen, R.M. (2007) Event-based climatology and typology of fog in the New York City region. *Journal of Applied Meteorology and Climatology*, 46, 1141–1168.
- Tyagi, S., Tiwari, S., Mishra, A., Singh, S., Hopke, P.K., Singh, S. and Attri, S. (2017) Characteristics of absorbing aerosols during winter foggy period over the National Capital Region of Delhi: impact of planetary boundary layer dynamics and solar radiation flux. *Atmospheric Research*, 188, 1–10.
- Van Schalkwyk, L. and Dyson, L.L. (2013) Climatological characteristics of fog at Cape Town international airport. *Weather and Forecasting*, 28, 631–646.
- Vautard, R., Yiou, P. and Van Oldenborgh, G.J. (2009) Decline of fog, mist and haze in Europe over the past 30 years. *Nature Geoscience*, 2, 115–119.
- Witiw, M.R. and LaDochy, S. (2008) Trends in fog frequencies in the Los Angeles Basin. *Atmospheric Research*, 87, 293–300.
- Yan, S., Zhu, B., Huang, Y., Zhu, J., Kang, H., Lu, C. and Zhu, T. (2020) To what extents do urbanization and air pollution affect fog? *Atmospheric Chemistry and Physics*, 20, 5559–5572.

SUPPORTING INFORMATION

Additional supporting information can be found online in the Supporting Information section at the end of this article.

How to cite this article: Smith, D. K. E., Dorling, S. R., Renfrew, I. A., Ross, A. N., & Poku, C. (2023). Fog trends in India: Relationships to fog type and western disturbances. *International Journal of Climatology*, 43(2), 818–836. <https://doi.org/10.1002/joc.7832>